DALTON
FULL PAPER

Reaction of di- and tri-valent chromium amides with O_2 †

Kamalesh B. P. Ruppa,[a] Khalil Feghali,[a] Istvan Kovacs,[a] Kasani Aparna,[a] Sandro Gambarotta,*[,a] Glenn P. A. Yap[b] and Corinne Bensimon[b]

[a] *Department of Chemistry, University of Ottawa, Ottawa, Ontario K1N 6N5, Canada*
[b] *Molecular Structure Center, University of Ottawa, Ottawa, Ontario K1N 6N5, Canada*

Homoleptic divalent $[\{Cr(NRR')\}_2(\mu\text{-}NRR')_2]\cdot 3thf$ (R = R′ = cyclohexyl **1a**; R = 3,5-$Me_2C_6H_3$, R′ = adamantyl **1b**) and trivalent chromium amides $[Cr(NRR')_3]$ (R = R′ = C_6H_{11} **2a**; R = 3,5-$Me_2C_6H_3$, R′ = adamantyl **2b**; RR′ = 2,2,6,6-$Me_4C_5H_6N$ **2c**) were synthesized by reaction of $[CrCl_2(thf)_2]$ or $[CrCl_3(thf)_3]$ with the appropriate amount of the corresponding lithium amide. All of these complexes, with the exception of **2c**, reacted with dioxygen to give the hexavalent chromium dioxo bis(amide) derivative, $[Cr(NRR')_2O_2]$ **4a** and **4b**. A possible intermediate $[\{Cr(NRR')_2\}_2(\mu\text{-}O)_2]\cdot C_6H_5Me$ was isolated by comproportionating **1b** with **4b**. A diamagnetic chromium(v) dimeric species, $[\{Cr(NRR')_2O\}_2(\mu\text{-}O)]$ **5b** was isolated upon treatment of **4b** with $P(C_6H_{11})_3$. The crystal structures of complexes **1b**, **2b**, **2c**, **3b**, **4a**, **4b** and **5b** have been determined.

Among transition-metal complexes in their highest oxidation states, hexavalent chromium species certainly display one of the most spectacular and wide-ranging reactivity patterns. These derivatives act as powerful oxidants for a variety of substrates including saturated and unsaturated hydrocarbons. For example, CrF_2O_2 is well known to ignite methane.[1] The dichloro analogue transforms saturated hydrocarbons into the corresponding halogenoalkanes under exceptionally mild reaction conditions.[2] Triflate (trifluoromethanesulfonate) derivatives oxidize a wide variety of organic substrates,[3] and $CrO_2(OR)_2$ is able to oxidize olefins.[4] Given this background, it is obvious that these systems are promising substrates to study the challenging topic of C–H bond activation of saturated hydrocarbons.[5] In addition, chromates find extensive application in metal-promoted organic synthesis.[6,7] In striking contrast with these features, high-valent oxochromium cyclopentadienyl derivatives,[8] including alkyls, are remarkably unreactive, probably as a result of a high degree of covalency of the Cr–C bond introduced by the π-donor ability of the cyclopentadienyl system.[8] Given these differences, it is not surprising that mechanistic and synthetic studies on the above systems were mainly directed to elucidate the pivotal role played by the nature of the ligand in determining the reactivity of these species.[2]

Since strong π donors such as the cyclopentadienyl ligand seem severely to subdue the reactivity of the metal center, we became interested in exploring the chemistry of high-valent chromium supported by weak π-donor ligands. It was hoped that by moderating the high reactivity of the metal center it would be possible to gain better control over its reactivity, thus making the behavior of these species more understandable. For this purpose, anionic organic amides were regarded as particularly promising. In addition to their weak π-donor ability, these ligands offer the possibility of adjusting both the steric hindrance and the electronic features around the transition metal *via* the appropriate selection of substituents on the nitrogen donor atom.[9]

As a synthetic pathway to high-valent oxochromium amide complexes, we have used chromium(II) amide complexes as starting materials for reactions with molecular oxygen. This choice was prompted by the exceptional sensitivity of these species to oxygen[10] and by the fact that the products of their oxidation have not been elucidated yet. In general, the interaction of chromium(II) complexes with dioxygen is expected to be a complex multistep reaction since the direct four-electron reduction of dioxygen by the same metal center is symmetry disallowed.[11] The reaction proceeds *via* formation of a superoxochromium(III) adduct[12] which probably reacts further to give oxidation of the metal center and cleavage of the O–O bond. By using sterically demanding amide ligands it was hoped to shed some light on the mechanism of the reaction of chromium(II) species with oxygen and to trap and isolate some of the intermediates. In order to gain insight into the mechanistic pathway of this reaction and related systems, the reactivity of chromium(III) amides with O_2 was also investigated.

Results and Discussion

Reaction of either $[CrCl_2(thf)_2]$ or $[CrCl_3(thf)_3]$ with 2 or 3 equivalents of LiNRR′ (R = R′ = C_6H_{11} **a**; R = 3,5-$Me_2C_6H_3$, R′ = adamantyl **b**) respectively led to the formation of the corresponding di- and tri-valent homoleptic chromium amides $[\{Cr(NRR')\}_2(\mu\text{-}NRR')_2]$ **1** and $[Cr(NRR')_3]$ **2** (Scheme 1). The reactions were significantly different in the case of the bulky Li(tmp) (tmp = 2,2,6,6-$Me_4C_5H_6N$ **c**). In this case reaction with either $[CrCl_2(thf)_2]$ or $[CrCl_3(thf)_3]$ afforded only $[Cr(tmp)_3]$ **2c** in low yield after work-up. In the case of complexes **2** the magnetic moments, calculated at room temperature, were consistent with the high-spin d^3 electronic configuration of the proposed formulation. The molecular structures of all these compounds were elucidated by X-ray analysis (see below).

The distortion of the molecular backbone observed in complex **1b** is unlikely to be caused by a significant Cr–Cr interaction. Probably it is the result of geometry or molecular packing optimization, since the Cr···Cr distance [Cr(1)···Cr(2) 2.85(1) Å] is only slightly longer than in complex **1a** [2.838(2) Å][13] which instead has a perfectly planar core. In any event, the

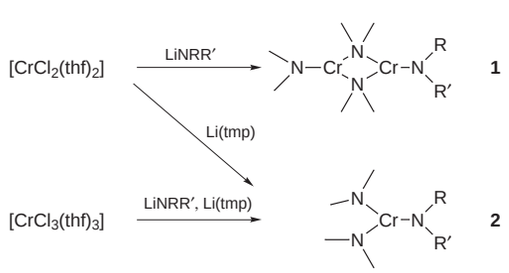

Scheme 1 R = R′ = C_6H_{11} **a**; R = 3,5-$Me_2C_6H_3$, R′ = adamantyl **b**; tmp = 2,2,6,6-$Me_4C_5H_6N$ **c**

† *Non-SI units employed*: $\mu_B \approx 9.27 \times 10^{-24}$ J T^{-1}, eV ≈ 1.60×10^{-19} J.

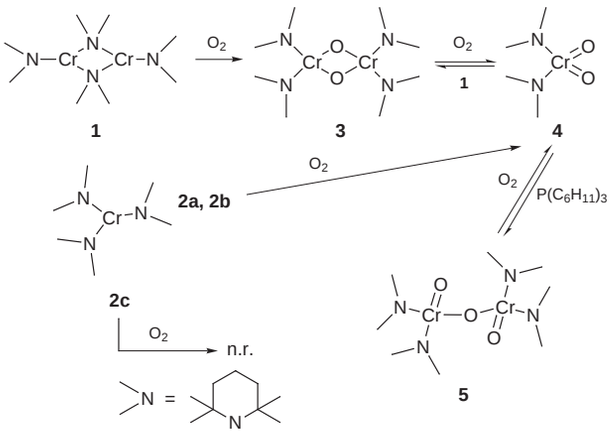

Scheme 2 n.r. = No reaction

Cr · · · Cr distances in the two complexes are rather long and unlikely to represent a significant bonding interaction. In contrast, the magnetic moments (μ_{eff} = 2.62 and 2.47 μ_B for **1a** and **1b** respectively) are low and consistent with the presence of less than two unpaired electrons per dimer, thus indicating the presence of a substantial magnetic coupling between the two metal centers.

With the exception of **2c**, compounds **1** and **2** readily react with dry oxygen. On exposure to dry oxygen, emerald-green solutions of [{Cr(NRR′)}$_2$(μ-NRR′)$_2$] **1a** or **1b** immediately turned brown and eventually intense blue after a few minutes. For both systems dark blue crystals of diamagnetic compounds were isolated in good yield from hexane upon cooling (Scheme 2). In all cases, combustion analysis data were consistent with the formulation [Cr(NRR′)$_2$O$_2$] (R = R′ = C_6H_{11} **4a**; R = 3,5-$Me_2C_6H_3$, R′ = adamantyl **4b**). Both the ^{1}H and the ^{13}C NMR spectra showed only one set of signals attributable to the ligand, thus suggesting the presence of fairly symmetric structures. A similar formulation, [Cr{N(SiMe$_3$)$_2$}$_2$O$_2$], was proposed for the bright yellow crystalline product obtained from the reaction of $CrCl_2O_2$ with $(Me_3Si)_2NH$.[14]

Complexes **4** were also obtained, *albeit* in lower yield, *via* treatment of the trivalent [Cr(NRR′)$_3$] **2a** and **2b** with O_2. Surprisingly, complex **2c** proved to be completely unreactive towards oxygen. No color change or indication of reaction could be observed upon thermolysis or photolysis of toluene solutions kept under an oxygen atmosphere for 1 week. Unchanged starting materials were invariably recovered in good yield. Conversely, as for complexes **1**, the reaction of **2a** or **2b** with O_2 was rapid and the solution changed almost immediately from brown to intense blue. In both cases, deep blue crystals of **4** were isolated and identified by comparison of the spectroscopic data with those of analytically pure samples. Similar to the case of the reaction of **2a** with sulfur,[15] the formation of **4** from **2** implies loss of one amide ligand. At this moment it is unclear how this is achieved. In the case of the reaction of [Cr(NPr$^i_2$)$_3$] with O_2, Bradley and co-workers[10c] proposed the formation of Pr$^i_2$NO, although the fate of the metal center was not clarified. We found no evidence for this process in our systems although this possibility cannot be definitely ruled out. The lack of reactivity of **2c** towards O_2 is surprising. On the other hand, the very large steric congestion around the metal center as well as the Cr · · · H 'agostic-like' interactions might well prevent even a small molecule like O_2 from approaching the metal center.

The occasional observation of the formation of a transient brown color during the reaction of complex **1** with O_2 before giving the blue dioxo-species **4** suggests that a reactive intermediate may be formed in the initial stage of the reaction. However, attempts to control the reaction by slowly feeding the reaction vessel with stoichiometric amounts of oxygen in toluene solution were not successful. Treatment of compounds **1** and **2** with milder oxidizing agents such as styrene oxide yielded intractable dark brown paramagnetic materials. However, reaction of **1b** with **4b** in toluene solution in a stoichiometric ratio 1:2 yielded paramagnetic [{Cr(NRR′)$_2$}$_2$(μ-O)$_2$]·C_6H_5Me **3b** (R = 3,5-$Me_2C_6H_3$, R′ = adamantyl) which was isolated as a brown crystalline material. The formula was indicated by combustion analysis data, while the magnetic moment was significantly lower than expected for a d^2 electronic configuration of tetravalent chromium. This is consistent with the presence of a dinuclear structure with some direct Cr–Cr interaction. Complex **3b** is very air sensitive and rapidly reacts with O_2 to give good yields of hexavalent **4**. Unfortunately, attempts to isolate and characterize the cyclohexyl analog **3a** yielded intractable materials.

In contrast to the hexavalent dioxochromium halide[2] and dialkoxide derivatives,[4a,d] complexes **4** are remarkably inert. These species do not react with olefins, such as styrene, ethylene and propylene, and do not oxidize simple organic substrates. Similar to the case of the cyclopentadienyl derivatives,[8] this unexpected stability is likely to be ascribed to the π-donating ability of the amide ligands which significantly quenches the redox potential of hexavalent chromium. Only in the case of treatment with P(C_6H_{11})$_3$ it was possible to abstract an oxygen atom from **4b** to form the diamagnetic derivative [{Cr(NRR′)$_2$O}$_2$(μ-O)] **5b**, which was isolated as a green crystalline material in good yield. The formulation was in agreement with combustion analysis data. The ^{1}H NMR spectrum shows the presence of only one ligand set thus indicating a fairly symmetric structure in solution.

In spite of the d^1 electronic configuration of pentavalent chromium and the absence of any apparent direct Cr–Cr interaction, complex **5b** is diamagnetic in both the solid state and solution. No significant variation of the chemical shifts was observed in the NMR spectra in the temperature range −80 to +80 °C. This observation is in line with previous literature data thus suggesting that the linear Cr–O–Cr array enables rather substantial magnetic coupling regardless of the oxidation state of the metal.[16]

The transformation of complex **1** into **4** is a four-electron process. In principle one could expect that the most energetically viable manner to obtain this transformation is through a one-step reaction. Divalent chromium might co-ordinate one molecule of O_2 and then simply transfer the four electrons necessary for cleavage of the O–O double bond to form the final product. However, theoretical work has indicated that this direct process is symmetry disallowed[11b] thus giving support to the idea that the reaction is indeed a multistep one.[11,12] It is well established that the preliminary stage is reversible formation of a 1:1 superoxochromium(III) adduct. Although its formation was clearly demonstrated only in aqueous solutions,[12] it is reasonable to assume that the same process might occur in a non-aqueous medium. Subsequent reaction of the superoxo intermediate with still unchanged chromium(II) starting material will form a dinuclear peroxochromium(III) complex, which through simple internal reorganization may lead to the formation of the chromium(IV) oxo-bridged species **3**. This process is probably the rate-determining step and almost certainly is irreversible.

Crystal structures

Complex 1b. Poor crystal quality and spontaneous loss of interstitial thf hampered the determination of the structure. This is reflected in the high values of the residuals. Complete anisotropic refinement was not possible for the two interstitial molecules of solvent due to positional and thermal disorder. Nevertheless, it was possible to obtain a mediocre quality structure sufficient to establish the connectivity. The structure is reminiscent of that previously reported for complex **1a**.[13] The core is composed of two three-co-ordinated chromium atoms

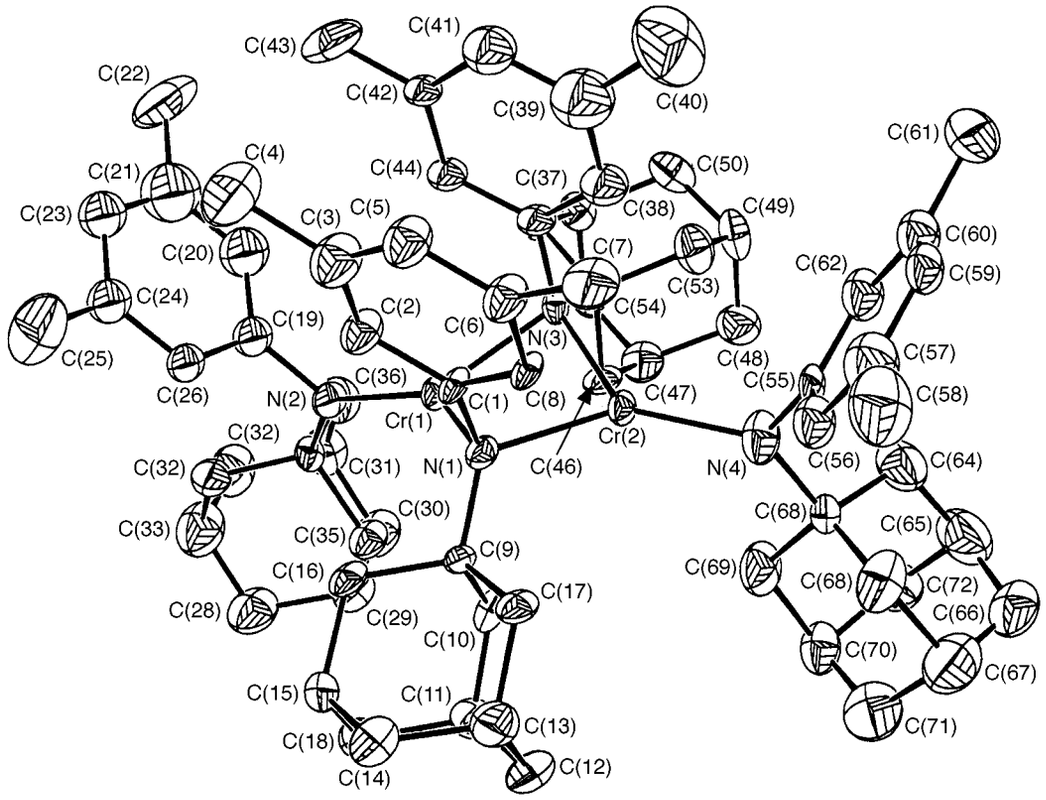

Fig. 1 An ORTEP[17] plot of complex **1b**. Thermal ellipsoids are drawn at the 30% probability level. Hydrogen atoms are omitted for clarity

bridged by two amide groups [Cr(1)–N(1) 2.08(2), Cr(1)–N(3) 2.07(2), Cr(2)–N(1) 2.07(2), Cr(2)–N(3) 2.10(2) Å] (Table 1). One terminal amide on each chromium atom [Cr(1)–N(2) 1.95(1), Cr(2)–N(4) 1.95(2) Å] completes the trigonal coordination sphere of each metal center [N(1)–Cr(1)–N(2) 139.0(7), N(1)–Cr(1)–N(3) 88.8(6), N(2)–Cr(1)–N(3) 131.9(7)°]. However, differently from the structure of **1a**, the N_4Cr_2 core is folded along the Cr–Cr axis in a saddle-shape conformation [N(1)–Cr(1)–N(3)–Cr(2) 24.0(3)°]. The two terminal nitrogen atoms are coplanar with the two metal centers and are placed at the same side of the intermetallic vector opposite to that occupied by the two bridging nitrogens (Fig. 1).

Complexes 2b, 2c. The molecular structures of the trivalent $[Cr(NRR')_3]$ **2b** and **2c** feature a nearly trigonal-planar geometry involving a chromium atom bonded to three nitrogen atoms of three amide ligands (Figs. 2 and 3). In both cases the chromium is slightly elevated above the plane containing the three nitrogens [0.25(5) and 0.23(5) Å respectively]. In the case of complex **2b** the three adamantyl groups of the three amide ligands are placed on the same side of the plane while the aromatic groups are situated on the opposite side. In **2c** the planes of the three rings are perpendicular to the CrN_3 core giving the molecule an overall 'paddlewheel' geometry. The coordination geometry around each of the three nitrogen atoms is trigonal planar [**2b**: N(1)–Cr–N(2) 121.76(8), N(1)–Cr–N(3) 116.96(8), N(2)–Cr–N(3) 120.74(8). **2c**: N(1)–Cr–N(2) 119.8(1), N(1)–Cr–N(3) 119.9(1), N(2)–Cr–N(3) 120.2(1)°] in both complexes thus suggesting the possibility of a significant N→Cr π donation. Indeed the Cr–N distances [**2b**: Cr–N(1) 1.855(2), Cr–N(2) 1.866(2), Cr–N(3) 1.882(2). **2c**: Cr–N(1) 1.907(3), Cr–N(2) 1.912(3), Cr–N(3) 1.929(3) Å] are noticeably short in spite of the considerable steric bulk of the amide ligand. The slightly longer distances observed in the case of **2c** may be attributed to larger steric hindrance. In this complex two methyl groups, pointing towards the metal center from above and below the molecular plane, form short contacts with the metal (C···H 2.60 Å). However, these 'agostic' interactions

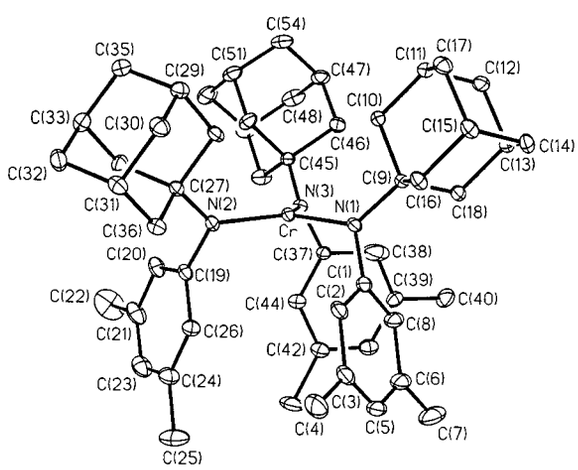

Fig. 2 An ORTEP plot of complex **2b**. Details as in Fig. 1

do not modify the high-spin electronic configuration of the metal center, which shows the expected value for the magnetic moment.

Complexes 4a, 4b. The two complexes possess a very similar structure; **4b** is located on a two-fold axis. In both cases the coordination sphere is defined by two nitrogen atoms of the two amide ligands and by the two oxygen atoms. The geometries about the chromium and nitrogen atoms are tetrahedral and trigonal planar respectively (Figs. 4 and 5). The Cr–O [Cr–O(1) 1.53(1), Cr–O(2) 1.613(9) **4a**; Cr–O(1) 1.591(2), Cr–O(1A) 1.591(2) Å **4b**] and Cr–N distances [Cr–N(1) 1.80(1), Cr–N(2) 1.82(1) **4a**; Cr–N(1) 1.847(2), Cr–N(1A) 1.847(2) Å **4b**] fall in the expected range and compare well with those of other oxochromium compounds containing amide ligands. The O–Cr–O angles [O(1)–Cr–O(2) 115.0(7) **4a** and O(1)–Cr–O(1A) 113.0(1)° **4b**] are wider than those observed in $[Cr(C_5H_5)MeO_2]$ [109.4(2)°][18] and $[CrO_2(OR)_2]$ [109.8(1)°].[4b] In both **4a** and **4b** the long O···O non-bonding distances [O(1)···O(2) 2.653(7)

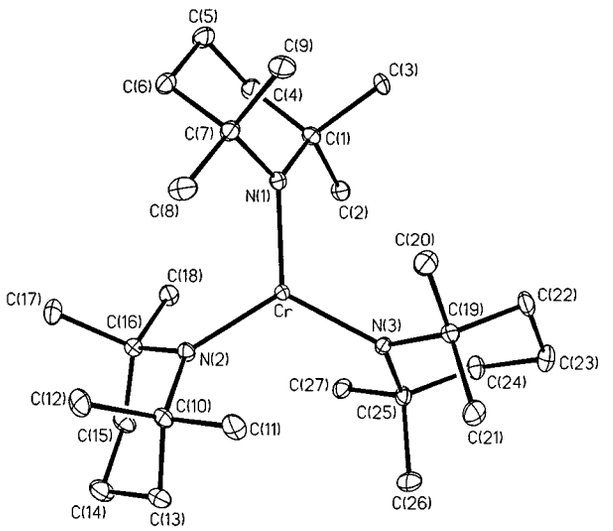

Fig. 3 An ORTEP plot of complex **2c**. Details as in Fig. 1

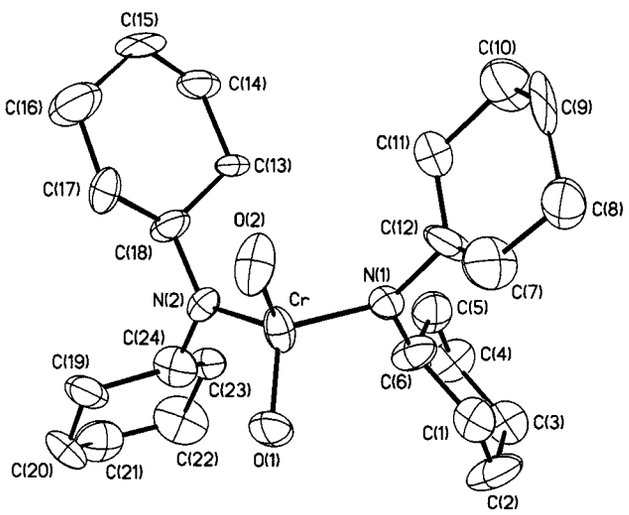

Fig. 4 An ORTEP plot of complex **4a**. Details as in Fig. 1

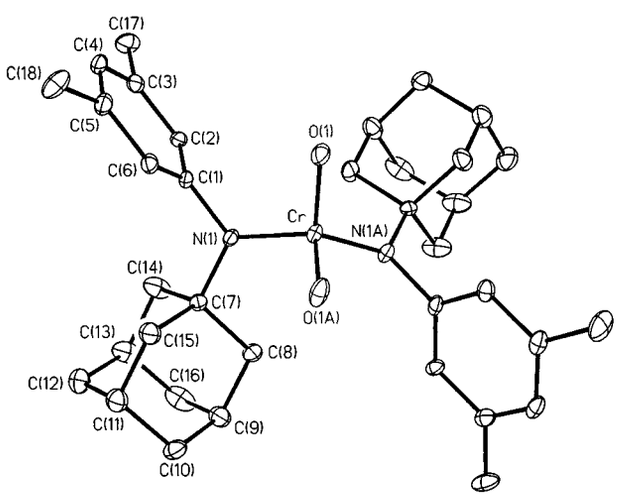

Fig. 5 An ORTEP plot of complex **4b**. Details as in Fig. 1

4a and O(1)···O(1A) 2.609(9) Å **4b**] rule out the formulation as tetravalent chromium peroxides.

Complex 3b. This compound is located on an inversion center. One adamantyl group was found rotationally disordered at an inversion center with a 75/25 site occupancy distribution. The components of the anisotropic displacement parameters of

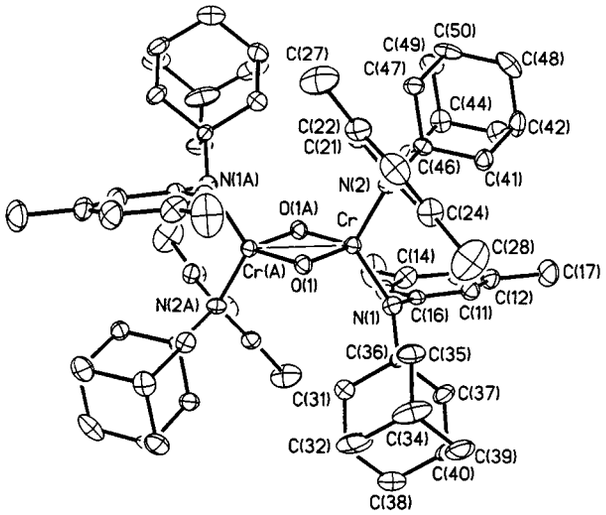

Fig. 6 An ORTEP plot of complex **3b**. Details as in Fig. 1

the disordered groups were restrained to be equal within an effective 0.01 standard deviation. All 1,2 and 1,3 distances in the disordered adamantyl group were restrained to be the same length for the corresponding atoms in the contributing conformations. One molecule of toluene was also located 50/50 disordered at an inversion center. The structure is formed by two identical $Cr(NRR')_2$ fragments bridged by two oxygen atoms (Fig. 6). The co-ordination geometry around each chromium is distorted tetrahedral [O(1)–Cr–N(1) 106.9(3), O(1)–Cr–N(2) 102.5(3), O(1)–Cr–O(1A) 90.2(2), O(1A)–Cr–N(1) 116.1(3), O(1A)–Cr–N(2) 115.5(3)°] and is defined by two nitrogen atoms of the two amide groups and two bridging oxygens. The distortion around chromium and the large N–Cr–N angle [N(1)–Cr–N(2) 119.4(3)°] are probably caused by the steric repulsion between the two amide ligands. The co-ordination geometry around each nitrogen atom is trigonal planar [Cr–N(1)–C(16) 108.9(5), Cr–N(1)–C(36) 130.6(6), C(16)–N(1)–C(36) 120.3(7)°] with rather short Cr–N distances [Cr–N(1) 1.852(7), Cr–N(2) 1.856(6) Å]. The Cr_2O_2 core is planar with rather short Cr–O distances [Cr–O(1A) 1.798(5), Cr–O(1) 1.804(5) Å] and narrow Cr–O–Cr angles [Cr–O(1)–Cr(A) 89.8(2)°]. The chromium centers are separated by a rather short distance [Cr–Cr(A) 2.543(3) Å] which is comparable to that of a vanadium analog[19] and might suggest the presence of a direct Cr–Cr interaction.

Complex 5b. The structure features a molecule placed on an inversion center with two tetrahedral $(R_2N)_2CrO$ fragments linked by a bridging oxygen with a linear Cr–O–Cr array [Cr–O(1)–Cr(A) 180°] (Fig. 7). Two nitrogen atoms of two amide ligands and one terminal oxygen atom complete the co-ordination sphere of each chromium atom. The geometry of the amide nitrogen atoms is trigonal planar as expected for terminally bonded amides with Cr–N bond distances [Cr–N(1) 1.863(3), Cr–N(2) 1.893(3) Å, Table 1] comparable to those of the other complexes reported in this work. The bridging Cr–O bond distance [Cr–O(1) 1.7660(6) Å] is slightly shorter than expected for a Cr–O single bond. The terminal chromium–oxygen bond distance [Cr–O(2) 1.591(3) Å] is very short, as expected, and comparable to those of **4a** and **4b**.

Molecular orbital calculations

As mentioned above, complexes **1a** and **1b** have fairly long Cr···Cr distances. Given the magnetic moments roughly indicative of two unpaired electrons per dimeric unit, a triplet state was considered to be a reasonable basis for the semi-empirical calculations.

There are several MOs of interest, which account for the Cr···Cr interaction in complex **1a**. The near degeneracy of the HOMO and HOMO-1 is rather pronounced (gap 0.04 eV) and accounts well for the observed paramagnetism. The HOMO (−8.65 eV) has the shape of a Cr–Cr σ bond and is formed by the overlap of hybrid combinations of chromium d atomic orbitals ($d_{x^2-y^2}$ and d_{z^2}) with a minor contribution from the p orbitals of the bridging nitrogen atoms (Scheme 3). The overlap is only marginal in spite of the favorable orientation and the MO should be considered as mainly non-bonding in character. Another weak Cr···Cr interaction (HOMO-8, −11.81 eV) is somewhat reminiscent of a Cr–Cr σ bond and is formed *via* overlap of the same hybrid combination of chromium d orbitals used in the HOMO but with a substantial mixing of the p_x atomic orbitals of the bridging nitrogen atoms. This interaction originates a large lobe distributed in the center of the Cr_2N_2 core. The most significant direct Cr–Cr σ interaction is realized with HOMO-36 (−23.05 eV) and is originated by the direct overlap of a hybrid combination of d_{z^2},4s orbitals of Cr. Even in this case the MO requires the substantial participation of the p_x orbitals of the bridging nitrogen atoms. Together, these Cr···Cr interactions account for only a very weak Cr···Cr bond (calculated bond order 0.3). The Cr–N–Cr bonding is mainly realized through several orbitals. Three are the most significant. The first (HOMO-4, −10.45 eV) is formed by overlap of the chromium d_{xz} atomic orbitals with the bridging nitrogen p_z. The orbital has two nodal planes bisecting the Cr_2N_2 plane along the N–N and Cr–Cr vectors. Another Cr–N–Cr σ bond is obtained with HOMO-9 (−12.04 eV) and is formed by interaction of the chromium d_{xz} orbitals lying on the molecular plane, with the coplanar p_x bridging nitrogen orbitals. In this case there is one nodal plane placed along the Cr–Cr vector. A relatively low-lying MO (HOMO-24, −15.45 eV) is a π-Cr–N–Cr bond. It is formed by the d_{xy} atomic orbitals of the two chromium atoms that mix with the p_y orbitals of the bridging nitrogen atoms, thus forming four lobes on the two sides of the molecular plane.

The deviation from planarity of the Cr_2N_2 core observed in complex **1b** and consequent lowering of the symmetry has important implications in the shape and distribution of the molecular orbitals. For simplicity, the adamantyl groups were replaced by Me groups while the methyls attached to the phenyl rings were replaced by hydrogen atoms. The calculation showed a relatively large HOMO − (HOMO-1) gap (0.29 eV) which, however, may still account for the paramagnetism observed at room temperature. Furthermore, calculations carried out for the same model compound on the singlet state gave a value of the relative energy three times higher thus supporting the choice of the triplet state as a basis. Among the frontier orbitals only HOMO-3 (−9.96 eV) is mainly chromium centered and accounts for some Cr···Cr interaction (Scheme 4). The orbital is originated by the overlap of two d_{z^2}/d_{yz} hybrid combinations of each chromium atom which form a sort of Cr–Cr σ bond by overlapping of the two lobes of the hybrid orbitals lying on the intermetallic vector. Similar to the case of the HOMO of complex **1a**, the overlap is rather minor and requires some participation of the bridging nitrogen atomic orbital. Thus the MO should probably be regarded as non-bonding with respect to the Cr···Cr interaction. The other two orbitals of interest mainly account for the bonding of the Cr_2N_2 core. The first (HOMO-27) had rather low energy (−16.18 eV) and it is mainly a Cr–N–Cr bond with a nodal plane along the N–N vector and perpendicular to the Cr_2N_2 core. It is realized *via* the overlap of two different hybrid combinations of d orbitals on the two Cr atoms (respectively d_{xy}/d_{xz} and $d_{x^2-y^2}/d_{z^2}$) with two different hybrid combinations of the two bridging nitrogen atom p orbitals (respectively p_x/p_y and p_x/p_z). Thus unusual 'twisted' shape of the MO is likely the result of the lack of symmetry and of the folding of the core. The last MO of interest (HOMO-34, −20.60 eV) is a fairly symmetric Cr–N–Cr σ bond. It is formed by the overlap of identical hybrid combinations of two d orbitals of the two Cr atoms which mix with the bridging nitrogen s orbitals and form two large delocalized lobes on the two Cr–N–Cr moieties. The overall calculated Cr–Cr bond order is smaller than in complex **1a** (0.19). This is obviously caused by the folding of the core (determined by steric factors) since the Cr···Cr distances of **1a** and **1b** are basically the same.

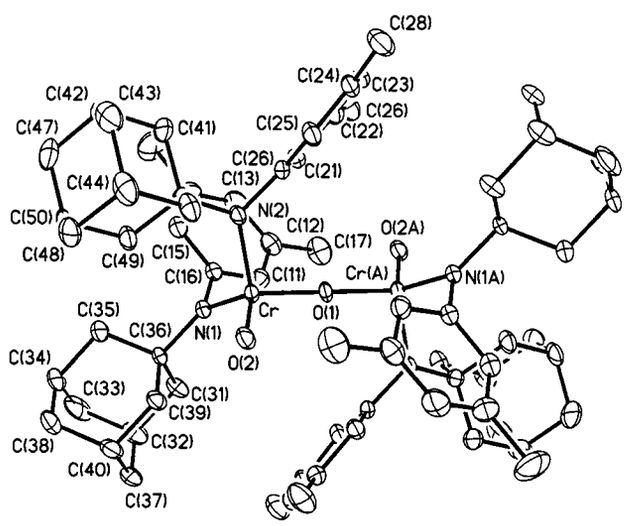

Fig. 7 An ORTEP plot of complex **5b**. Details as in Fig. 1

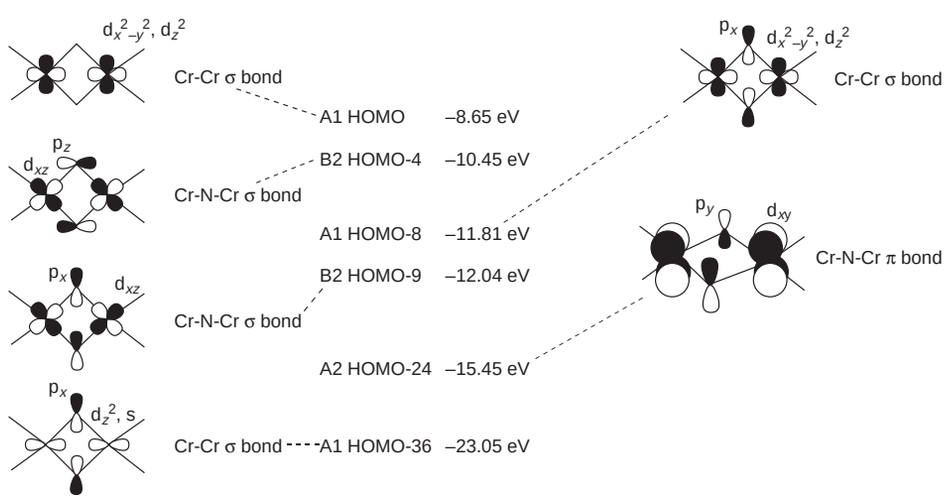

Scheme 3

Table 1 Selected bond distances (Å) and angles (°) for complexes **1b**, **2b**, **2c**, **3b**, **4a**, **4b** and **5b**

1b		**2b**		**2c**		**3b**		**4a**		**4b**		**5b**	
Cr(1)–Cr(2)	2.85(1)	Cr–N(1)	1.855(2)	Cr–N(1)	1.907(3)	Cr–Cr(A)	2.543(3)	Cr–O(1)	1.53(1)	Cr–O(1)	1.591(2)	Cr–O(1)	1.7660(6)
Cr(1)–N(1)	2.08(2)	Cr–N(2)	1.866(2)	Cr–N(2)	1.912(3)	Cr–O(1)	1.804(5)	Cr–O(2)	1.613(9)	Cr–O(1A)	1.591(2)	Cr–O(2)	1.591(3)
Cr(1)–N(2)	1.95(1)	Cr–N(3)	1.8815(19)	Cr–N(3)	1.929(3)	Cr–O(1A)	1.798(5)	Cr–N(1)	1.80(1)	Cr–N(1)	1.847(2)	Cr–N(1)	1.863(3)
Cr(1)–N(3)	2.07(2)	N(1)–C(1)	1.448(3)	N(1)–C(1)	1.490(5)	Cr–N(1)	1.852(7)	Cr–N(2)	1.82(1)	Cr–N(1A)	1.8469(19)	Cr–N(2)	1.893(3)
Cr(2)–N(1)	2.07(2)	N(1)–C(9)	1.479(3)	N(1)–C(7)	1.505(5)	Cr–N(2)	1.856(6)	N(1)–C(12)	1.44(2)	N(1)–C(1)	1.449(3)	O(1)–Cr(1A)	1.7661(6)
Cr(2)–N(3)	2.10(2)	N(2)–C(19)	1.440(3)			N(1)–C(16)	1.45(1)	N(1)–C(6)	1.44(2)	N(1)–C(7)	1.509(3)	N(1)–C(16)	1.446(5)
Cr(2)–N(4)	1.95(2)	N(2)–C(27)	1.477(3)			N(1)–C(36)	1.51(1)	N(2)–C(24)	1.45(2)			N(1)–C(36)	1.514(5)
N(1)–C(1)	1.50(2)	N(3)–C(37)	1.434(3)			N(2)–C(26)	1.44(1)	N(2)–C(18)	1.44(2)			N(2)–C(26)	1.439(5)
N(1)–C(9)	1.49(2)	N(3)–C(45)	1.479(3)			N(2)–C(46)	1.49(1)					N(2)–C(46)	1.520(5)
N(2)–C(27)	1.47(2)												
N(2)–C(19)	1.47(2)												
N(1)–Cr(1)–N(2)	139.0(7)	N(1)–Cr–N(2)	121.76(8)	N(2)–Cr–N(1)	119.8(1)	O(1A)–Cr–O(1)	90.2(2)	O(1)–Cr–O(2)	115.0(7)	O(1)–Cr–O(1A)	113.0(1)	Cr–O(1)–Cr(A)	180.0
N(1)–Cr(1)–N(3)	88.8(6)	N(1)–Cr–N(3)	116.96(8)	N(2)–Cr–N(3)	120.2(1)	O(1A)–Cr–N(2)	115.5(3)	O(1)–Cr–N(1)	109.8(6)	O(1)–Cr–N(1)	104.79(8)	O(1)–Cr–O(2)	109.0(1)
N(1)–Cr(2)–N(3)	88.4(6)	N(2)–Cr–N(3)	120.74(8)	N(3)–Cr–N(1)	119.9(1)	O(1A)–Cr–N(1)	116.1(3)	O(2)–Cr–N(1)	106.5(5)	O(1)–Cr–N(1A)	110.73(9)	O(2)–Cr–N(1)	115.6(1)
N(1)–Cr(2)–N(4)	136.6(8)	Cr–N(1)–C(1)	112.4(1)	Cr–N(1)–C(7)	122.2(2)	N(1)–Cr–N(2)	119.4(3)	O(1)–Cr–N(2)	106.7(5)	O(1A)–Cr–N(1)	110.73(9)	O(1)–Cr–N(1)	110.7(1)
N(2)–Cr(1)–Cr(2)	166.9(7)	Cr–N(1)–C(9)	129.7(2)	Cr–N(1)–C(1)	123.1(2)	O(1)–Cr–N(1)	106.9(3)	O(2)–Cr–N(2)	106.3(6)	O(1A)–Cr–N(1A)	104.79(8)	O(2)–Cr–N(2)	107.7(2)
Cr(1)–Cr(2)–N(4)	167.9(8)	C(1)–N(1)–C(9)	117.6(2)	C(1)–N(1)–C(7)	114.4(3)	O(1)–Cr–N(2)	102.5(3)	N(1)–Cr–N(2)	112.7(4)	N(1)–Cr–N(1A)	112.98(9)	O(1)–Cr–N(2)	103.6(1)
N(3)–Cr(1)–N(2)	131.9(7)					N(1)–Cr–Cr(A)	121.2(2)	Cr–N(1)–C(6)	114(1)	Cr–N(1)–C(1)	116.66(15)	N(1)–Cr–N(2)	109.6(1)
N(3)–Cr(2)–N(4)	134.7(8)					Cr(A)–Cr–N(2)	117.2(2)	Cr–N(1)–C(12)	129(1)	Cr–N(1)–C(7)	123.94(14)	C(16)–N(1)–Cr	112.0(2)
Cr(1)–N(1)–Cr(2)	86.8(6)					Cr(A)–O(1)–Cr	89.8(2)	C(6)–N(1)–C(12)	117(1)	C(1)–N(1)–C(7)	115.6(2)	C(16)–N(1)–C(36)	116.7(3)
Cr(1)–N(3)–Cr(2)	86.4(6)					Cr–N(1)–C(16)	108.9(5)					C(36)–N(1)–Cr	131.2(3)
						Cr–N(1)–C(36)	130.6(6)						

The intermetallic distance in complex **3b** is substantially shorter than in **1**, as a probable result of the higher oxidation state of the metal. Molecular orbital calculations were carried out on the atomic coordinates constrained to C_{2v} symmetry. Again, the triplet state was used as a basis to account for the observed paramagnetism. The small gap between the HOMO (−7.45 eV) and HOMO-1 (−7.66 eV) nicely accounts for the observed paramagnetism. There are four MOs responsible for the direct Cr–Cr interaction (Scheme 5). The orbital HOMO-3 (−9.02 eV) is a very weak Cr–Cr σ bond. the bond is realized *via* a marginal overlap of the two lobes of d_{z^2},d_{yz} hybrid combinations of each chromium atom lying on the intermetallic vector. The bridging oxygen atoms contribute to some extent to the formation of the MO by using the hybrid combinations p_x/p_y. The other three are much lower in energy. The first is again a sort of Cr–Cr σ bond (HOMO-32, −16.84 eV) and is realized with the overlap of the lobes of the $d_{x^2-y^2}$,d_{yz} hybrid combinations placed on the intermetallic vector, with a hybrid p_z,p_y combination of the bridging oxygen atoms. This MO forms a large lobe delocalized in the center of the Cr_2O_2 core. The same hybrid combination with participation of the p_y orbitals of the bridging oxygen atoms is used for the next MO (HOMO-33, −17.02 eV) to originate a weak Cr–Cr σ bond. A Cr–Cr π bond (HOMO-34, −17.10 eV) is originated by the overlap of the d_{xy} orbitals of the two chromium atoms with a strong participation of the bridging oxygen p_y orbitals. The MO thus consists of two rather symmetric lobes on the two sides of the Cr_2O_2 core. These four MOs result in an overall Cr–Cr bond order of 0.4, higher than in complexes **1a** and **1b**. The bonding of the Cr_2O_2 core is realized mainly with four MOs. The first (HOMO-16, −13.51 eV) is a Cr–O–Cr σ bond formed by direct overlap of d_{xz} orbitals of the chromium atoms with the p_z of the bridging oxygen. This gives two lobes uniformly distributed on the two Cr–O–Cr moieties and separated by a nodal plane which bisects the core along the Cr–Cr vector. The second MO (HOMO-20, −13.95 eV) is responsible for the Cr–O–Cr π bond. The overlap is originated by the chromium d_{yz} atomic orbitals with the p_y oxygen orbitals thus forming four lobes symmetrically placed on the two sides and above and below the plane of the Cr_2O_2 core. This orbital possesses two nodal planes that are respectively the molecular plane and its orthogonal, which perpendicularly bisects the core along the Cr–Cr vector. Another orbital (HOMO-25, −15.74) is also a Cr–O–Cr σ bond. It is originated by interaction of the chromium d_{xz} orbitals with a hybrid combination p_x, p_z of the bridging oxygen atoms, forming two nodal planes along the O–O and Cr–Cr vectors which perpendicularly bisect the Cr_2O_2 plane. The last orbital of interest (HOMO-30, −16.23 eV) is also a Cr–O–Cr σ bond formed by interaction of chromium hybrid d_{z^2},$d_{x^2-y^2}$ combinations with the p_x orbitals of the bridging oxygen atoms. Different from HOMO-25, this has only one nodal plane along the O–O vector.

Questions arise about how an efficient coupling in complex **5** is realized *via* the bridging oxide atom, which is placed in the middle of the intermetallic vector and should act as a shield between the two metal centers. This is particularly puzzling given that the oxo-bridged species **3b** with two bent Cr–O–Cr arrays is paramagnetic in spite of having a much shorter Cr···Cr distance. Therefore, the linear arrangement Cr–O–Cr must necessarily be responsible for providing an efficient pathway to couple electrons. Calculations carried out on the atomic coordinates of **5b** showed a remarkably large HOMO − LUMO gap (7.02 eV) which is largely sufficient to account for the observed diamagnetism. The HOMO (−8.27 eV) is a Cr-centered molecular orbital with strong d character and nonbonding with respect to the Cr–O–Cr moiety (Scheme 6). Five molecular orbitals account for the Cr–O–Cr bonding interaction. The first, HOMO-8 (−14.61 eV), is a largely delocalized π bond. It is formed by hybrid combinations of d_{xz} and d_{xy} atomic orbitals on each chromium atom with a hybrid combination (p_y/p_z) of the bridging oxygen atom, thus forming two lobes alongside the Cr–O–Cr framework. The two terminal oxygen atoms are also involved in the formation of the MO by using hybrid combinations of their p_y/p_z atomic orbitals. The MO has two parallel nodal planes, each bisecting one chromium atom and perpendicular to the O–Cr–O–Cr–O plane. The next MO of interest (HOMO-15, −15.99 eV) is also a largely delocalized π system very similar in shape to the previous one. However, the π bonding between the two chromium atoms and the bridging oxygen is realized mainly *via* the interaction of the p_y/p_z hybrid combinations of the oxygen with two

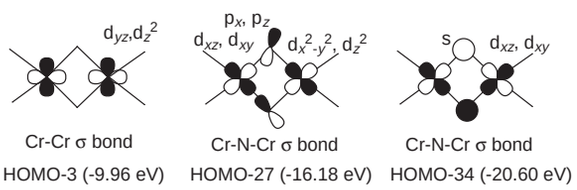

Scheme 4

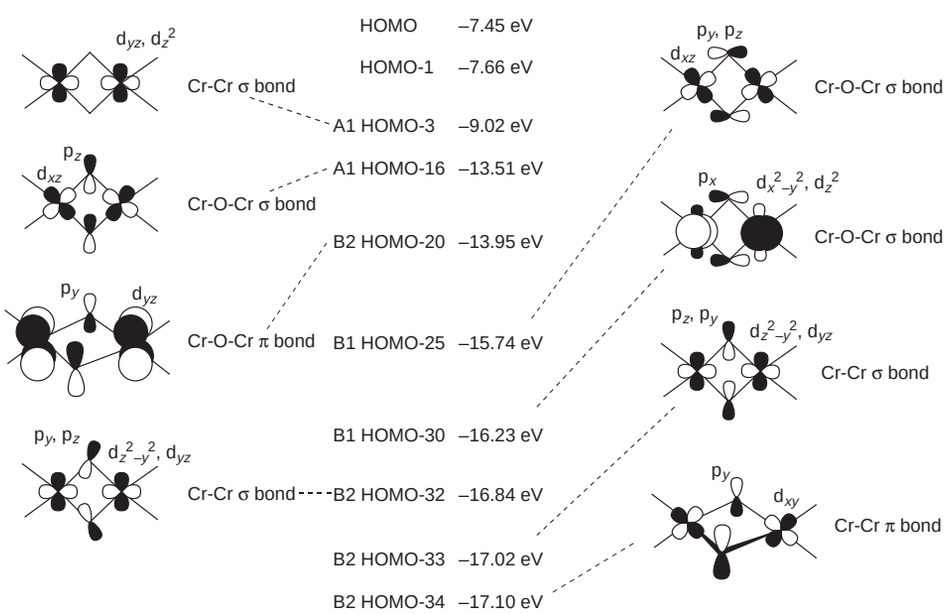

Scheme 5

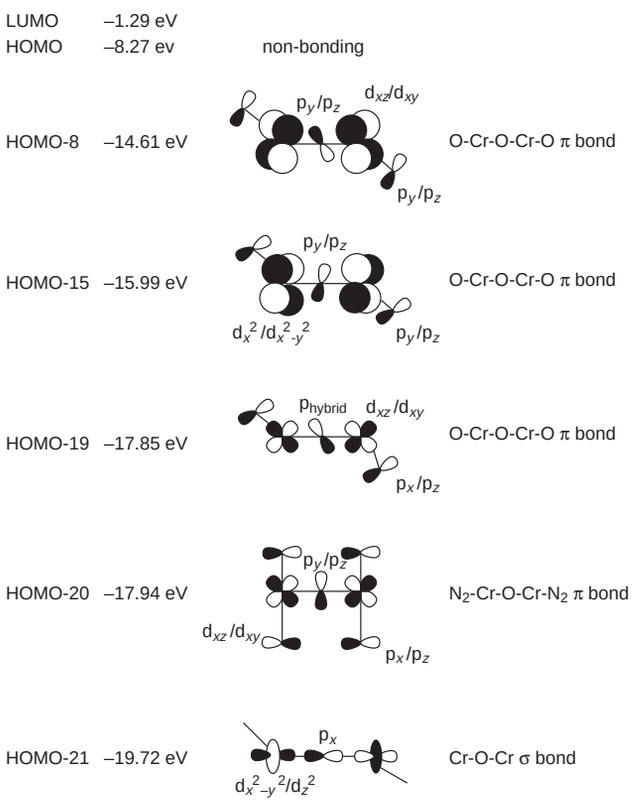

Scheme 6

$d_{z^2}/d_{x^2-y^2}$ hybrid combinations of the d orbitals of each chromium atom. This orbital also encompasses the terminal oxo atoms by using in-phase combinations of their p_y/p_z orbitals thus forming two lobes alongside the O–Cr–O–Cr–O backbone and on the two sides of the O–Cr–O–Cr–O plane. The next MO (HOMO-19, −17.85 eV) is also an O–Cr–O–Cr–O π bond. Its shape is similar to that of HOMO-15. The orbital is formed by hybrid combinations of the three p orbitals of the central O atom and hybrid combinations of d_{xz} and d_{xy} orbitals of each chromium atom. The two terminal oxygens use mainly p_x/p_z hybrids and form two large and well delocalized lobes alongside the molecular backbone. Another Cr–O–Cr π bond (HOMO-20) was located at −17.94 eV and is formed by the overlap of a d_{xy}, d_{xz} hybrid combination of the chromium atoms with the p_y/p_z hybrid of the central O atom. This orbital however encompasses the four terminal amide nitrogen atoms again forming two couples of largely delocalized lobes alongside the two N–Cr–O–Cr–N frameworks. The last MO of interest (HOMO-21, −19.72 eV) is a regular Cr–O–Cr σ bond generated by the p_x orbital of the bridging oxygen with a combination of the $d_{x^2-y^2}$ and d_{z^2} atomic orbitals of each chromium atom to form two lobes lying symmetrically on the Cr–O–Cr vector. The orbital has a nodal plane perpendicular to the Cr–O–Cr vector and bisecting the bridging O atom. As a result of the presence of a considerable number of MOs distributed along the O–Cr–O–Cr–O backbone, the Cr–(μ-O) bond order is remarkably high (1.56) and nicely explains the diamagnetism of the molecule.

Conclusion

With this work it was possible to clarify the fate of the reaction of chromium-(II) and -(III) amides with dioxygen. Some of the intermediates were isolated and characterized, thus partially contributing to clarifying the mechanism of oxidation of the amides. However, the fact that complex **3** may be obtained *via* comproportionation of the dioxo **4** with the divalent **1** through a rapid and quantitative reaction cannot be taken as a proof for the hexavalent **4** being formed *via* disproportionative elimination of Cr^{II} from the dinuclear **3**, since the reaction of **3** with O_2 to give **4** is also a very fast process. Conversely, complex **5** does not react with O_2 to form **4** at an appreciable rate, thus indicating that this species is not an intermediate in the formation of **4** from either **1** or **2**.

The inertness of the chromium(VI) amide derivatives towards the oxidation of organic substrates is intriguing and remarkably contrasts with the high reactivity observed for the chlorinated analogs. This is probably due to a fairly good π-donor ability of the amide ligands which, similar to the case of the cyclopentadienyl systems, significantly quench the Lewis acidity of the metal center. In this respect, the alkoxide derivatives will probably provide a reactivity pattern intermediate between that of the high-valent halogenated derivatives and the amides and perhaps will give a key to a better understanding of the remarkable reactivity of high-valent chromium species.

Experimental

All operations were performed under an inert atmosphere by using standard Schlenk techniques. The complexes $[CrCl_2(thf)_2]$,[20] **1a**,[13] **2a**[15] and LiNRR′·Et_2O (R = 3,5-$Me_2C_6H_3$, R′ = adamantyl)[21] were prepared according to published procedures. The compound Li(tmp) was prepared in hexane by treating a solution of 2,2,6,6-tetramethylpiperidine with 2.5 M $LiBu^n$ solution at −80 °C. Solvents were dried with appropriate drying agents and distilled prior to use. Oxygen gas was dried over phosphorus pentaoxide. Infrared spectra were recorded on a Mattson 9000 FTIR instrument from Nujol mulls prepared in a dry-box. Samples for magnetic susceptibility measurements were prepared inside a dry-box and sealed into calibrated tubes; measurements were carried out with a Gouy balance (Johnson Matthey) at room temperature. The magnetic moment were calculated by standard methods,[22a] and corrections for underlying diamagnetism were applied.[22b] Elemental analyses were carried out with a Perkin-Elmer 2400 CHN analyzer. Ratios between heavy atoms were determined by X-ray fluorescence by using a Philips 2400 instrument. Semiempirical PM3 calculations were carried out on a Silicon Graphics workstation by using the program SPARTAN 4.0.[23] The program's default parameters were used in the calculations carried out on the atomic coordinates of the complexes as obtained from the crystal structure determinations. In the case of **1a** and **3b**, the geometry was slightly optimized to introduce the C_{2v} symmetry.

Preparations

[{Cr(NRR′)}$_2$(μ-NRR′)$_2$]·3thf 1b (R = 3,5-$Me_2C_6H_3$, R′ = adamantyl). A suspension of $[CrCl_2(thf)_2]$ (3.4 g, 12.9 mmol) in thf (150 cm^3) was stirred with LiNRR′·Et_2O (8.7 g, 25.9 mmol) at room temperature. The mixture slowly turned emerald green. After stirring for 2 d at room temperature the solvent was removed *in vacuo*. The residue was extracted with thf (100 cm^3) and the extract filtered to eliminate a small amount of insoluble material. The resulting solution was concentrated to nearly 30 cm^3, diethyl ether (50 cm^3) added and allowed to stand at −30 °C for 2 d upon which emerald-green crystals of complex **1b** separated (4.5 g, 3.4 mmol, 53%). IR (Nujol mull, NaCl, cm^{-1}): 1587s, 1351s, 1343m, 1304s, 1288s, 1183m, 1150s, 1106m, 1081s, 1026m, 987w, 978w, 950m, 924m, 909m, 843s, 817w, 710m, 686s, 676m, 650w and 625m. μ_{eff} = 2.47 μ_B. Satisfactory elemental analyses could not be obtained due to the extreme sensitivity of the crystalline samples.

[Cr(NRR′)$_3$] 2b (R = 3,5-$Me_2C_6H_3$, R′ = adamantyl). A solution of $[CrCl_3(thf)_3]$ (1.8 g, 4.8 mmol) in thf (125 cm^3) was treated with LiNRR′ (5.1 g, 15.2 mmol) at ambient temperature. The mixture rapidly changed to dark greenish brown. It

was stirred for 8 h and then evaporated to dryness. The residue was extracted with thf (100 cm^3) and then filtered to eliminate LiCl. The clean solution was concentrated and mixed with ether (100 cm^3). The resulting solution was cooled to −30 °C and allowed to stand for 2 d at low temperature, upon which crystals of complex **2b** separated (2.5 g, 2.9 mmol, 61%) [Found (Calc. for $C_{54}H_{72}CrN_3$): C, 79.22 (79.56); H, 8.92 (8.90); N, 4.57 (5.15)%]. IR (NaCl, Nujol mull, cm^{-1}): 1587s, 1351m, 1342w, 1298s, 1186w, 1160s, 1110s, 1089s, 1031m, 994s, 953s, 923s, 848m, 842m, 814w, 792w, 709m and 691s. $\mu_{eff} = 3.97\ \mu_B$. FAB mass spectrum: *m*/*z* 815.5 (L_3Cr^+), 560.3 (L_2Cr^+) and 307.1 (LCr^+).

[Cr(2,2,6,6-Me$_4$C$_5$H$_6$N)$_3$] 2c. *Method A.* A suspension of $[CrCl_2(thf)_2]$ (2.1 g, 7.7 mmol) in thf (100 cm^3) was treated with solid Li(tmp) (2.3 g, 15.5 mmol) at room temperature. The solution changed immediately to green and gradually to purple. After stirring for 1 d at room temperature the solvent was removed *in vacuo*. The solid residue was extracted with diethyl ether (100 cm^3) and the extract filtered to eliminate a small amount of green solid. The resulting solution was concentrated to nearly 50 cm^3 and cooled to −30 °C for 1 d resulting in the precipitation of purple crystals of **2c** (0.4 g, 0.8 mmol, 11%). IR (Nujol mull, NaCl, cm^{-1}): 1359m, 1339w, 1283m, 1227s, 1196m, 1164s, 1125s, 1054w, 990m, 964s, 924m, 900s, 860s and 739m. $\mu_{eff} = 4.23\ \mu_B$ [Found (Calc. for $C_{27}H_{54}CrN_3$): C, 68.53 (68.60); H, 11.39 (11.51); N, 8.73 (8.89)%].

Method B. A suspension of $[CrCl_3(thf)_3]$ (1.7 g, 4.5 mmol) in diethyl ether (150 cm^3) was treated with Li(tmp) (2.0 g, 13.4 mmol). The solution turned dark green and slowly to purple. It was stirred at ambient temperature for 48 h, filtered to remove LiCl, concentrated to 50 cm^3 and cooled at −30 °C for 12 h to obtain dark purple crystals of **2c**. Yield 0.5 g, 1.2 mmol (26%). The product was identified by comparison of its IR spectrum and magnetic moment with those of an analytically pure sample.

[Cr{N(C$_6$H$_{11}$)$_2$}$_2$O$_2$] 4a. *Method A.* A suspension of $[CrCl_3(thf)_3]$ (3.7 g, 9.9 mmol) in toluene (100 cm^3) was stirred with $LiN(C_6H_{11})_2$ (5.5 g, 29.4 mmol) at −30 °C. After stirring for 2 h the solvent was removed *in vacuo* and the residue extracted with hexane (200 cm^3). The solution was filtered and the resulting brown solution exposed to dry oxygen upon which it gradually changed to dark blue. The mixture was stirred for 8 h under an atmosphere of oxygen, filtered and evaporated to dryness. The solid was redissolved in toluene and cooled to −30 °C for 8 h. Dark blue crystals of **4a** separated {1.5 g, 3.4 mmol, 34% based on $[CrCl_3(thf)_3]$} [Found (Calc. for $C_{24}H_{44}CrN_2O_2$): C, 64.85 (64.83); H, 9.99 (9.98); N, 6.47 (6.30)%]. IR (Nujol mull, NaCl, cm^{-1}): 1661–1609w (br), 1463s, 1343m, 1324w, 1260s, 1158w, 1143m, 1099s, 1080s, 1028s, 1020s, 986s, 974m, 959s, 937w, 925s, 915m, 890m, 843m, 806m, 788m, 739w and 710w. ^{1}H NMR (C_6D_6, 20 °C, 500 MHz): δ 1.07 (br s, 4 H, *para*), 1.25 (br s, 8 H, *meta*), 1.52 (br s, 4 H, *para*), 1.73 (br s, 16 H, *ortho* and *meta*), 1.79 (br s, 8 H, *ortho*) and 3.85 (m, 4 H, *ipso*). ^{13}C NMR (C_6D_6, 20 °C, 125.7 MHz): δ 25.5 (*p*-C of C_6H_{11}), 26.3 (*m*-C of C_6H_{11}), 33.9 (*o*-C of C_6H_{11}) and 69.9 (*ipso*-C of C_6H_{11}) ppm. FAB(+) mass spectrum: *m*/*z* 445 (5, M^+) and 182 {100%, $[(C_6H_{11})_2NH_2^+]$}.

Method B. A solution of $[\{Cr[N(C_6H_{11})_2]\}_2\{\mu\text{-}N(C_6H_{11})_2\}_2]$ (1.3 g, 1.6 mmol) in toluene (90 cm^3) was evacuated and flushed with dry oxygen. It changed from green to brown and finally became dark blue. It was filtered and concentrated to 30 cm^3. After standing for 8 h at −30 °C, dark blue crystals of complex **4a** were obtained (0.8 g, 1.8 mmol, 56%). The product was identified by comparison of the analytical and spectroscopic data with those of an analytically pure sample.

[Cr(NRR′)$_2$O$_2$] 4b (R = 3,5-Me$_2$C$_6$H$_3$, R′ = adamantyl). *Method A.* A brownish green solution of $[Cr(NRR')_3]\cdot Et_2O$ (2.1 g, 2.4 mmol) in toluene (100 cm^3) was exposed to an excess of dry oxygen. The solution changed instantly to dark blue. It was stirred for 8 h under oxygen and then evaporated to dryness. The solid residue was extracted with hexane (100 cm^3). Upon standing for 24 h at room temperature dark blue crystals of complex **4b** were obtained (0.7 g, 1.2 mmol, 50%) [Found (Calc. for $C_{36}H_{48}CrN_2O_2$): C, 72.88 (72.93); H, 8.02 (8.18); N, 4.81 (4.73)%]. IR (Nujol mull, NaCl, cm^{-1}): 1601m, 1583s, 1354w, 1300s, 1288s, 1261m, 1190w, 1149m, 1102m, 1063s, 1045m, 1026s, 983m, 968m, 955s, 926s, 888w, 847w, 801m, 707w and 696m. ^{1}H NMR (C_6D_6, 20 °C, 500 MHz): δ 6.68 (br s, 3 H, aryl), 2.15 (s, 6 H, Me, aryl), 2.01 (br s, 6 H, CH_2, adamantyl), 1.95 (br s, 3 H, CH, adamantyl) and 1.44 (br s, 6 H, CH_2, adamantyl). ^{13}C NMR (C_6D_6, 20 °C, 125.7 MHz): δ 156.3 (1 C, C^1 of aryl), 137.7 (2 C, $C^{3,5}$ of aryl), 124.7 (3 C, $C^{2,4,6}$ of aryl), 67.6 (1 C, quaternary C of adamantyl), 44.5 (3 C, CH_2, adamantyl), 36.8 (3 C, CH_2, adamantyl), 30.9 (3 C, CH, adamantyl) and 21.7 (2 C, Me, aryl).

Method B. A solution of complex **1** (1.0 g, 0.7 mmol) in toluene (50 cm^3) was exposed to dry oxygen. It changed from emerald green to reddish brown and finally became dark blue. The mixture was stirred for 8 h under an atmosphere of dry oxygen and then evaporated to dryness. The residue was extracted with hexane (80 cm^3). Dark blue crystals of complex **4b** were obtained upon standing at ambient temperature for 24 h (0.7 g, 1.21 mmol, 80%). The product was identified by comparison of the analytical and spectroscopic data with those of an analytically pure sample.

Method C. Crystalline complex **3b** was dissolved in C_6D_6 in a 5 mm Teflon screw-capped NMR tube. The solution was frozen, evacuated and flushed with dry oxygen. Upon warming to room temperature the initial deep reddish brown solution changed to dark blue. The NMR spectrum showed the presence of **4b** as the only reaction product.

[{Cr(NRR′)$_2$}$_2$(μ-O)$_2$]·C$_6$H$_5$Me 3b (R = 3,5-Me$_2$C$_6$H$_3$, R′ = adamantyl). Complex **4b** (2.0 g, 3.4 mmol) was added to an emerald-green solution of **1b** (1.9 g, 1.4 mmol) in thf (100 cm^3). The solution slowly changed to dark reddish brown. After 24 h of stirring at room temperature it was evaporated to dryness. Upon extraction with toluene (100 cm^3), concentration and cooling to −30 °C, dark brown crystals of **3b** were obtained (1.7 g, 1.4 mmol, 43%) [Found (Calc. for $C_{79}H_{104}Cr_2N_4O_2$): C, 75.97 (76.17); H, 8.56 (8.42); N, 4.41 (4.50)%]. IR (Nujol mull, NaCl, cm^{-1}): 1597m, 1582s, 1354m, 1343w, 1302s, 1261s, 1186w, 1150s, 1104s, 1079s, 1026s, 996s, 954w, 926s, 847m, 802s, 709w, 691s and 608s. ^{1}H NMR (C_6D_6, 20 °C, 200 MHz): δ 6.74 (br s, 3 H, aryl), 3.26 (br s, CH_2, Et_2O), 2.36 (br s, 6 H, CH_2, adamantyl), 2.20 (br s, 6 H, CH_3, aryl), 1.89 (br s, 3 H, CH, adamantyl), 1.61 (br s, 6 H, CH_2, adamantyl) and 1.12 (br s, CH_3, Et_2O). $\mu_{eff} = 1.44\ \mu_B$.

[{Cr(NRR′)$_2$O}$_2$(μ-O)] 5b (R = 3,5-Me$_2$C$_6$H$_3$) R′ = adamantyl). A dark blue solution of complex **4b** (1.7 g, 2.7 mmol) in toluene (80 cm^3) was treated with $P(C_6H_{11})_3$ (1.7 g, 6.0 mmol) at ambient temperature. Within a few minutes it changed to dark green. After 8 h of stirring the solvent was evaporated *in vacuo* and the residue extracted with diethyl ether (100 cm^3). The solution was filtered and allowed to stand at ambient temperature for 24 h upon which dark green crystals of **5b** were obtained (1.1 g, 0.9 mmol, 69%) [Found (Calc. for $C_{72}H_{96}Cr_2N_4O_3$): C, 74.23 (73.94); H, 8.32 (8.27); N, 4.88 (4.79)%]. IR (Nujol mull, NaCl, cm^{-1}): 1599s, 1582s, 1354s, 1343m, 1296s, 1193w, 1185w, 1155m, 1120w, 1106m, 1098w, 1067s, 1045s, 1029s, 991w, 975s, 957s, 930s, 916s, 891w, 878m, 845s, 819m, 794w, 761m, 708s and 691s. ^{1}H NMR (C_6D_6, 20 °C, 500 MHz): δ 8.56 (br s, 2 H, 2,6-CH, aryl), 6.70 (s, 1 H, 4-CH, aryl), 3.25 (q, CH_2, Et_2O), 3.15 (br s, 6 H, CH_2, adamantyl), 2.32 (s, 6 H, CH_3, aryl), 1.68 (q, 6 H, CH_2, adamantyl), 1.25 (s, 3 H, CH, adamantyl) and 1.11 (t, CH_3, Et_2O).

Table 2 Crystal data and structure analysis results

	1b	**2b**	**2c**	**3b**	**4a**	**4b**	**5b**
Formula	$C_{84}H_{120}Cr_2N_4O_3$	$C_{54}H_{72}CrN_3$	$C_{27}H_{54}CrN_3$	$C_{79}H_{104}Cr_2N_4O_2$	$C_{24}H_{44}CrN_2O_2$	$C_{36}H_{48}CrN_2O_2$	$C_{72}H_{96}Cr_2N_4O_3$
M	1337.87	815.15	472.73	1245.66	444.61	592.76	1169.53
Lattice	Orthorhombic	Monoclinic	Monoclinic	Triclinic	Orthorhombic	Monoclinic	Triclinic
Space group	$P2_12_12_1$	$P2_1/c$	$P2_1/n$	$P\bar{1}$	$P2_12_12_1$	$C2/c$	$P\bar{1}$
a/Å	21.779(8)	18.7868(2)	7.7585(1)	11.568(2)	12.7811(4)	23.8166(4)	10.9576(5)
b/Å	22.448(6)	12.5147(3)	17.8418(2)	12.667(3)	13.8499(3)	7.2580(2)	12.0511(6)
c/Å	15.253(6)	20.7613(4)	19.3185(2)	13.035(3)	13.8973(4)	20.5043(4)	13.5151(7)
α/°				90.852(2)			111.616(1)
β/°		108.720(2)	92.932(1)	107.622(2)		118.407(1)	92.442(6)
γ/°				108.403(2)			100.894(1)
U/Å^3	7457(4)	4623.0(2)	2670.67(5)	1714.4(6)	2460.1(1)	3117.6(1)	1616.9(1)
Z	4	4	4	1	4	4	1
T/K	115	173	173	298	298	173	298
D_c/g cm^{-3}	1.192	1.171	1.176	1.207	1.20	1.263	1.201
μ/cm^{-1}	3.4	2.9	4.5	3.7	4.86	4.0	3.85
F(000)	2896	1764	1044	670	968	1272	628
R, R'	0.091, 0.152	0.052, 0.063	0.066, 0.115	0.089, 0.194	0.077, 0.195	0.036, 0.045	0.060, 0.140
Goodness of fit	3.78	2.13	2.11	1.11	1.08	1.79	1.19

Mo-Kα radiation (λ 0.710 73 Å); $R = \Sigma(F_o - F_c)/\Sigma F_o$, $R' = [\Sigma(F_o - F_c)^2/\Sigma wF_o^2]^{\frac{1}{2}}$. All structures refined against F excluding **3b**, **4a** and **5b** which were refined against F^2, $R'(F^2) = [\Sigma(F_o^2 - F_c^2)^2/\Sigma(wF_o^2)^2]^{\frac{1}{2}}$.

X-Ray crystallography

Data were collected at −158 °C using the ω–2θ scan technique to a maximum 2θ value of 50.0° for suitable air-sensitive crystals mounted with viscous oil on glass fibers on the goniometer head of either a Siemens CCD or Rigaku instrument. Cell constants and orientation matrices were obtained from the least-squares refinement of carefully centered reflections from 50 initial data frames. Redundant reflections were averaged using redundant data at different effective azimuthal angles. Data were corrected for Lorentz-polarization effects and for absorption. The structures were solved by direct methods. With the exception of complexes **1b** and **3b**, the positions of all the non-hydrogen atoms were refined anisotropically. Hydrogen atoms were introduced at their idealized positions. The final cycle of full-matrix least-squares refinement was based on the number of observed reflections with $I > 2.5\sigma(I)$. All calculations were performed either by using the SHELXTL (version 5.03) or NRCVAX software packages. Details of the crystal data and structure solution are given in Table 2.

CCDC reference number 186/930.

Acknowledgements

This work was supported by the National Science and Engineering Council of Canada (NSERC) through an operating grant; NATO is also gratefully acknowledged for a travel grant.

References

1 A. Engelbrecht and A. V. Grosse, *J. Am. Chem. Soc.*, 1952, **74**, 5262.
2 G. K. Cook and J. M. Mayer, *J. Am. Chem. Soc.*, 1995, **117**, 7139; 1994, **116**, 1855; K. B. Sharpless, A. Y. Teranishi and J. E. Backvall, *J. Am. Chem. Soc.*, 1987, **99**, 3120.
3 J. W. Suggs and L. Ytuarte, *Tetrahedron Lett.*, 1986, **27**, 437.
4 (*a*) L. M. Baker and W. L. Carrick, *J. Org. Chem.*, 1970, **35**, 774; (*b*) P. Stavropoulos, N. Bryson, M. T. Youinou and J. A. Osborn, *Inorg. Chem.*, 1990, **29**, 1807; (*c*) W. J. Behr and J. Fuchs, *Z. Naturforsch.*, 1973, **286**, 597; (*d*) F. J. Feher and R. L. Blanski, *J. Chem. Soc.*, *Chem. Commun.*, 1990, 1614; (*e*) S. L. Chadha, V. Sharma and A. Sharma, *J. Chem. Soc.*, *Dalton Trans.*, 1987, 1253.
5 R. A. Sheldon and J. K. Kochi, *Metal-Catalyzed Oxidation of Organic Compounds*, Academic Press, New York, 1981; J. A. Davies, P. L. Watson, J. F. Liebman and A. Greenberg, *Selective Hydrocarbon Activation*, *Principles and Progress*, VCH, New York, 1990; C. L. Hill, *Activation and Functionalization of Alkanes*, Wiley, New York, 1989; A. E. Shilov, *Activation of Saturated Hydrocarbons by Transition Metal Complexes*, D. Reidel, Dordrecht, 1984; D. J. Hucknall, *Selective Oxidation of Hydrocarbons*, Academic Press, New York, 1974; J. Halpern, *Fundamental Research in Homogeneous Catalysis*, ed. A. E. Shilov, Gordon and Breach, New York, 1986, vol. 1, p. 393; R. H. Crabtree, *Chem. Rev.*, 1985, **85**, 245; A. Sen, *Acc. Chem. Res.*, 1988, **21**, 421.
6 M. R. Pressprich, R. D. Willett, W. W. Paudler and G. L. Gard, *Inorg. Chem.*, 1990, **29**, 2872; M. R. Pressprich, R. D. Willett, R. D. Poshusta, S. C. Saunders, H. B. Davis and G. L. Gard, *Inorg. Chem.*, 1988, **27**, 260.
7 J. Muzart, *Chem. Rev.*, 1992, **92**, 113 and refs. therein; F. Freeman, *Chem. Rev.*, 1975, **75**, 439.
8 R. A. Heintz, R. L. Ostrander, A. L. Rheingold and K. H. Theopold, *J. Am. Chem. Soc.*, 1994, **116**, 11 387; D. B. Morse, T. B. Rauchfuss and S. R. Wilson, *J. Am. Chem. Soc.*, 1988, **110**, 8234; B. J. Thomas, S. K. Noh, G. K. Schulte, S. C. Sendlinger and K. H. Theopold, *J. Am. Chem. Soc.*, 1991, **113**, 893; B. J. Thomas and K. H. Theopold, *J. Am. Chem. Soc.*, 1988, **110**, 5902; K. H. Theopold, *Acc. Chem. Res.*, 1990, **23**, 263.
9 D. C. Bradley, M. B. Hursthouse, K. M. A. Malik and R. Moseler, *Transition Met. Chem.* (*Weinheim*), 1978, **3**, 253 and refs. therein; M. F. Lappert, P. P. Power, A. R. Sanger and R. C. Srivastava, *Metal and Metalloid Amides*, Ellis Horwood, Chichester, 1980 and refs. therein; G. Wilkinson, *Comprehensive Coordination Chemistry*, Pergamon, Oxford, 1987; W. E. Buhro, M. H. Chisholm, K. Folting, J. C. Huffman, J. D. Martin and W. E. Streib, *J. Am. Chem. Soc.*, 1992, **114**, 557 and refs. therein; T. P. Blatchford, M. H. Chisholm and J. C. Huffman, *Inorg. Chem.*, 1987, **26**, 1920.
10 (*a*) D. C. Bradley, M. B. Hursthouse and C. W. Newing, *Chem. Commun.*, 1971, 411; (*b*) E. C. Alyea, J. S. Basi, D. C. Bradley and M. H. Chisholm, *Chem. Commun.*, 1968, 495; (*c*) J. C. W. Chien, W. Kruse, D. C. Bradley and C. W. Newing, *Chem. Commun.*, 1970, 1177.
11 (*a*) S. N. Brown and J. M. Mayer, *Inorg. Chem.*, 1992, **31**, 4091; (*b*) M. A. Lockwood, P. E. Fanwick, O. Eisenstein and I. P. Rothwell, *J. Am. Chem. Soc.*, 1996, **118**, 2762.
12 A. Bakac, S. L. Scott, J. H. Espenson and K. R. Rodgers, *J. Am. Chem. Soc.*, 1995, **117**, 6483; M. E. Brynildson, A. Bakac and J. H. Espenson, *J. Am. Chem. Soc.*, 1987, **109**, 4579.
13 J. J. H. Edema, S. Gambarotta, A. Meetsma, A. L. Spek, W. J. J. Sweets and M. Y. Chiang, *J. Chem. Soc.*, *Dalton Trans.*, 1993, 789; *Inorg. Chem.*, 1989, **28**, 812.
14 H. W. Lam, G. Wilkinson, B. Hussain-Bates and M. B. Hursthouse, *J. Chem. Soc.*, *Dalton Trans.*, 1993, 1477.
15 D. Reardon, I. Kovacs, K. B. P. Ruppa, K. Feghali, S. Gambarotta and J. Petersen, *Chem. Eur. J.*, 1997, **3**, 1482.
16 B. G. Gafford, R. A. Holwerda, H. J. Schugar and J. A. Potenza, *Inorg. Chem.*, 1988, **27**, 1126; B. G. Gafford, C. O'Rear, J. H. Zhang, C. J. O'Connor and R. A. Holwerda, *Inorg. Chem.*, 1989, **28**, 1720; M. Yevitz and J. A. Stanko, *J. Am. Chem. Soc.*, 1971, **93**, 1512; M. D. DiVaira and F. Mani, *Inorg. Chem.*, 1984, **23**, 409; A. R. Barron, J. E. Salt, G. Wilkinson, M. Motevalli and M. B. Hursthouse, *J. Chem. Soc.*, *Dalton Trans.*, 1987, 2947.

17 C. K. Johnson, ORTEP, Report ORNL-5138, Oak Ridge National Laboratory, Oak Ridge, TN, 1976.
18 S. K. Noh, R. A. Heintz, B. S. Haggerty, A. L. Rheingold and K. H. Theopold, *J. Am. Chem. Soc.*, 1992, **114**, 1892.
19 M. Moore, K. Feghali and S. Gambarotta, *Inorg. Chem.*, 1997, **36**, 2191.
20 F. H. Köhler and W. Prössdorf, *Z. Naturforsch.*, *Teil B*, 1977, **32**, 1026.
21 K. B. P. Ruppa, N. Desmangles, S. Gambarotta, G. Yap and A. L. Rheingold, *Inorg. Chem.*, 1997, **36**, 1194.
22 (*a*) M. B. Mabbs and D. J. Machin, *Magnetism and Transition Metal Complexes*, Chapman and Hall, London, 1973; (*b*) G. Foese, C. J. Gorter and L. J. Smits, *Constantes Selectionnées Diamagnetisme*, *Paramagnetisme*, *Relaxation Paramagnetique*, Masson, Paris, 1957.
23 SPARTAN 4.0, Wavefunction, Inc., Irvine, CA, 1995.
24 G. Sheldrick, SHELXTL version 5.03, Madison, WI, 1994.

Received 17*th November* 1997; *Paper* 7/08229K